Frequency-Freezing FLL for Enhanced Synchronization Stability of Grid-Following Converters during Grid Faults

Taul, Mads Graungaard; Wang, Xiongfei; Davari, Pooya; Blaabjerg, Frede

Published in:
2020 IEEE 21st Workshop on Control and Modeling for Power Electronics (COMPEL)

DOI (link to publication from Publisher):
10.1109/COMPEL49091.2020.9265841

Publication date:
2020

Document Version
Accepteret manuscript, peer-review version

Citation for published version (APA):
Taul, M. G., Wang, X., Davari, P., & Blaabjerg, F. (2020). Frequency-Freezing FLL for Enhanced Synchronization Stability of Grid-Following Converters during Grid Faults. I *2020 IEEE 21st Workshop on Control and Modeling for Power Electronics (COMPEL)* (s. 1-7). IEEE (Institute of Electrical and Electronics Engineers). https://doi.org/10.1109/COMPEL49091.2020.9265841

Frequency-Freezing FLL for Enhanced Synchronization Stability of Grid-Following Converters during Grid Faults

Mads Graungaard Taul, Xiongfei Wang, Pooya Davari, Frede Blaabjerg
Dept. of Energy Technology, *Aalborg University*
Aalborg, Denmark
mkg@et.aau.dk, xwa@et.aau.dk, pda@et.aau.dk, fbl@et.aau.dk

***Abstract*—Transient instability is an issue for grid-following converters operating under grid faults when complying with low-voltage ride-through requirements. This has initiated much research with the aim to understand, model, and prevent loss of synchronization for synchronous-reference frame phase-locked loop (SRF-PLL)-synchronized systems. However, as the majority of grid faults are asymmetrical, a more complex synchronization unit is needed for the extraction of voltage sequences and phase tracking. This paper proposes a method for enhanced transient stability during severe grid faults for more complex synchronization structures designed to deal with asymmetrical fault conditions. This is done by freezing the frequency of a stationary-reference frame frequency-locked loop. The global asymptotic stability of the method is mathematically proven, and its performance is experimentally verified. Based on the mathematical equivalence between frequency-locked loops and phase-locked loops, it is shown that the presented method can be generalized to both stationary-reference and synchronous-reference frame structures and can, therefore, be a suitable solution in a wide range of applications.**

I. Introduction

The synchronization dynamics of grid-connected power converters are known to have a large impact on the stability and fault ride-through performance under grid faults [1]–[3]. Up till now, the modeling of converter large-signal synchronization stability [2], [4]–[8] has paved the way for numerous enhanced control methods [9]–[16]. All these control methods are developed based on the assumption that the grid fault is symmetrical. However, this is rarely the case in reality [17], and hence, a simple synchronous-reference frame phase-locked loop (SRF-PLL) can no longer be applied for the converter control since the synchronization control needs to be able to extract the sequence components of the asymmetrical grid voltage and then perform the phase tracking. It also makes the modeling more cumbersome and raises the question of how to enhance the transient instability of grid-following converters operated under asymmetrical grid faults. To address this, a globally asymptotically stable synchronization unit is proposed, which is capable of handling both symmetrical and asymmetrical grid faults. The main contributions of the paper can be summarized in the following points:

1) Proposing a frequency-freezing control for frequency-locked loops (FLLs) to enhance synchronization stability during asymmetrical and symmetrical grid faults.
2) Providing a mathematical proof for global asymptotic stability of the proposed method using Lyapunov theory.
3) By showing a mathematical equivalence between the used dual reduced-order generalized integrator frequency-locked loop (DROGI-FLL) and a SRF-PLL structure, it is identified that the stability enhancement using the frequency-freezing control is equivalent to setting the integral gain of a SRF-PLL type structure to zero during the fault, as it has been previously proposed [13], [28]. Therefore, this work gives a unification of this control method for stationary-reference frame FLLs and rotating-reference frame PLLs.

The remainder of this article is structured as follows: The studied system and the proposed control method are described in Section II. Following this, the dq-reference frame equivalence between the DROGI-FLL and an SRF-PLL type structure is presented in Section III. The large-signal stability of the proposed method is analyzed in Section IV, which is verified numerically in Section V during different grid faults. The proposed control is experimentally validated in Section VI and the paper is finally concluded in Section VII.

II. System under Study and Proposed Strategy

A grid-following converter is considered for this study, which is shown in Fig. 1. The converter output is connected to the grid through a line impedance, Z_L, where the fault location for symmetrical and asymmetrical faults is indicated with a red arrow connected to ground. During asymmetrical faults, methods to extract the sequence voltages include the dual second-order generalized-integrator PLL/FLL (DSOGI-PLL/FLL) [18], [19], the decoupled double SRF-PLL (DDSRF-PLL) [20], or a multiple complex-coefficient filter PLL (MCCF-PLL) [21], among different types of FLLs [22].

For this work, the grid-following structure in Fig. 1 uses a DROGI-FLL [23], to extract the sequence voltage components at the point of common coupling (PCC). The converter-side currents are controlled using a proportional-resonant (PR)

This work was supported by the Reliable Power Electronic-Based Power System (REPEPS) project at the Department of Energy Technology, Aalborg University as a part of the Villum Investigator Program funded by the Villum Foundation.

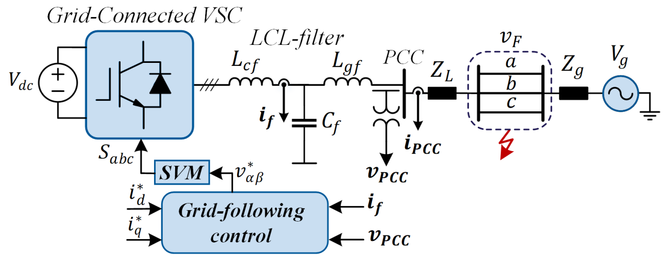

Fig. 1. Structure of grid-following converter connected to the grid where grid faults are considered to occur at v_F. SVM: Space Vector Modulation.

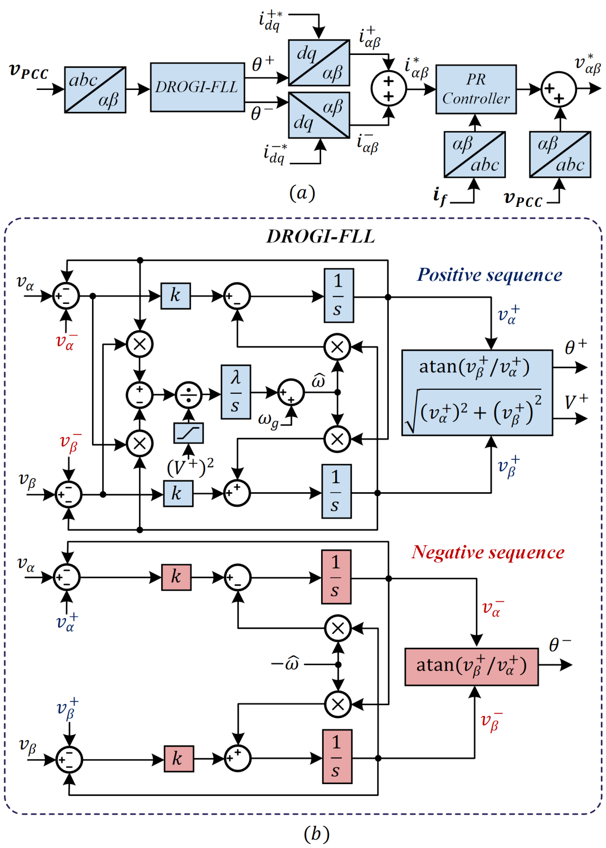

Fig. 2. Grid-following control used for converter. (a): Complete outlook of the grid-following control shown in Fig. 1. (b): Detailed view of the DROGI-FLL used for sequence extraction and synchronization.

controller with the PCC voltage feed-forward for improved dynamic response. i_d^* is set to 1 per-unit (pu) under normal operating conditions whereas i_q^* is calculated based on the required dynamic voltage support from the considered grid code. According to a German grid code for installation in the medium-voltage network [24], a grid-connected converter should be able to operate under severe low-voltage conditions and inject dual-sequence currents during asymmetrical faults. This is required, since as shown in [25], overvoltages can be averted by injecting negative sequence currents during asymmetrical faults.

To analyze the large-signal synchronization stability, the PCC voltage in the positive-sequence frame can be expressed

TABLE I
MAIN PARAMETERS OF THE GRID-FOLLOWING CONVERTER.

Symbol	Description	Physical Value
S_N	Nominal power	2.5 kVA
V_N	Nominal grid voltage	$200 \cdot \sqrt{3}$ V
I_N	Nominal converter current	$6/\sqrt{2}$ A
V_g	RMS grid phase voltage	200 V
f_n	Nominal frequency	50 Hz
V_{dc}	dc-link voltage	730 V
L_{cf}	Converter-side inductor	5 mH
L_{gf}	Grid-side inductor	3 mH
C_f	Filter capacitor	20 μF
f_{sw}	Switching frequency	10 kHz
f_s	Sampling frequency	10 kHz
Z_L	Line impedance	0.23 + 0.073j pu
Z_g	Grid impedance	0.1 pu
$K_{p,ic}$	Proportional gain PR controller	10 Ω
$K_{r,ic}$	Resonant gain of PR controller	1000 Ω/s
$K_{r,ic}$	Resonant gain of PR controller	1000 Ω/s
ω_N	DROGI-FLL tuning	35 rad/s

as

$$V_{PCC}^{+}\mathrm{e}^{\mathrm{j}\theta^{+}} = V_F^{+}\mathrm{e}^{\mathrm{j}\theta_F^{+}} + Z_{LT}\mathrm{e}^{\mathrm{j}\phi_{LT}^{+}} I^{+}\mathrm{e}^{\mathrm{j}\theta_C^{+}} \tag{1}$$

where $\theta_C^{+} = \theta^{+} + \theta_I^{+}$, Z_{LT} and ϕ_{LT} are the combined line and transformer impedance magnitude and phase, respectively, and $\theta_{PCC}^{+} = \theta^{+}$ prior to the fault. Uppercase letters represent vector magnitudes. Multiplying both sides of (1) with $\mathrm{e}^{-\mathrm{j}\theta^{+}}$ and taking the imaginary part gives

$$v_q^{+} = V_F^{+}\sin\left(\theta_F^{+} - \theta^{+}\right) + Z_{LT} I^{+}\sin\left(\phi_{LT}^{+} + \theta_I^{+}\right). \tag{2}$$

During normal operating conditions where $\theta^{\pm} = \theta_{PCC}^{\pm}$ then $v_q^{+} = 0$. To achieve stable synchronization after a disturbance, one must be able to control $v_q^{+} = 0$. This means that the following must be satisfied

$$I^{+} \leq \frac{-V_F^{+}\sin\left(\theta_F^{+} - \theta^{+}\right)}{Z_{LT}\sin\left(\phi_{LT}^{+} + \theta_I^{+}\right)} \implies I^{+} \leq \frac{V_F^{+}}{\left|Z_{LT}\sin\left(\phi_{LT}^{+} + \theta_I^{+}\right)\right|}, \tag{3}$$

which represents the necessary stability condition for current injection in the positive-sequence frame. By replacing the superscript $+$ with $-$, the negative sequence stability limit is achieved. During pure reactive current injection, the necessary stability condition in (3) is reduced to

$$I^{+} \leq \frac{V_F^{+}}{R_L}. \tag{4}$$

The limit in (3) is only a necessary condition for stability, whereas the transient stability when the fault occurs or voltage recovers is strongly dependent on the dynamics of the synchronization unit and its associated damping. The DROGI-FLL, as depicted in Fig. 2(b), has two control parameters, k, λ, which are selected as $k = 2\omega_N/\sqrt{2}$ and $\lambda = \omega_N^2$. Here, the damping ratio has the relationship $\zeta \propto \frac{1}{\omega_N^2}$, which indicates that high damping can be provided by selecting a high value for k or a low value for λ. Yet, which value should be selected to guarantee the transient stability is unknown and it is dependent on the severity of the fault and the converter injection. One may sweep through a large number of fault conditions with different controller parameters to estimate the critical damping ratio [26]. However, this may be difficult to do in practice since a realistic value of the worst-case fault condition is difficult to estimate. Therefore, to enhance the transient synchronization stability without identifying the needed critical damping, it is proposed to freeze the frequency of the DROGI-FLL. This is done by setting $\lambda = 0$ during a fault, which provides infinite damping, which is sufficient for a stable synchronization process, given the existence of a stable operating point.

III. Dq-frame Equivalence of DROGI-FLL

The design and stability analysis for FLL-based synchronization units are fundamentally different from that of synchronous-reference frames PLLs. In general, an FLL is a stationary-reference frame adaptive recursive filter, which is constructed using second-order generalized integrators in the case of real-coefficient filters (RCF) or reduced-order generalized integrators in the case of a complex coefficient bandpass/notch filter (CCF) [23], [27]. The FLL uses a band-pass filter to extract the positive and negative sequence fundamental voltage components and these band-pass filters are then made frequency-adaptive by employing a frequency detector, i.e., the frequency adaptive loop. With the above and since the similarity between FLL-based and PLL-based structures are not immediately obvious due to the large visual difference, it is desired to investigate the stability of an FLL synchronization unit while showing its equivalence in the more commonly used dq-reference frame.

To that end, since the necessary stability condition from (3) is developed in the rotating-reference frame, it is more intuitive to establish a mathematically-equivalent dq-frame representation of the DROGI-FLL. In this way, the presented analysis is not limited to the DROGI-FLL, but may be used with any synchronization unit following the same procedure.

In [18, Section V.B], it is demonstrated that an SRF-PLL with amplitude normalization and frequency estimation in the integral path (See Fig. 8(a) in [22]) is mathematically equivalent to a single ROGI-FLL. Therefore, the DROGI-FLL shown in Fig. 2(b) can be understood as two parallel SRF-PLLs rotating at the fundamental positive and negative frequencies, as shown in Fig. 3. Notice from Fig. 2 that the fundamental positive-sequence component extracted by the first equivalent SRF-PLL in the DROGI-FLL is subtracted from the input of the second SRF-PLL, and the extracted fundamental negative-sequence component by the second SRF-PLL is subtracted from the input of the first one. Notice also that the second SRF-PLL does not estimate the frequency itself, and the center frequency of its voltage-controlled oscillator (VCO) is adapted to frequency changes using the frequency estimated by the first SRF-PLL. Now, the cross feed-back network between the sequence frames in Fig. 2(b) can be simply transferred into the dq-reference frame by applying the Park transformation, as shown in the equivalent structure in Fig. 3. This representation

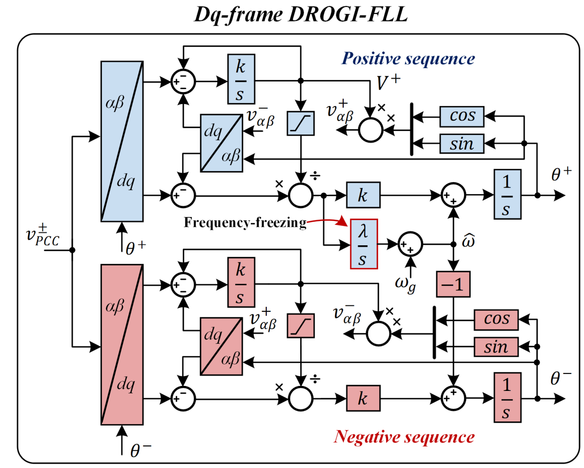

Fig. 3. Equivalent dq-frame representation of DROGI-FLL shown in Fig. 2(b). The location of the frequency-freezing control ($\lambda = 0$) is highlighted.

is the corresponding SRF-PLL structure of the DROGI-FLL, which is used for stability analysis and can be used to visualize the equivalence between different stationary-reference frame methods and synchronous-reference frame methods.

IV. Proof of Stability Enhancement

Taking the derived equivalent dq-frame representation of the DROGI-FLL shown in Fig. 3, one can write for the positive-sequence frame that

$$\theta^+ = \int \omega_g + \frac{k}{V^+}\left(v_q^+ - V^- \sin\!\left(\theta^+ - \theta^-\right)\right) dt. \quad (5)$$

where

$$V^+ = k \int \left(v_d^+ - V^+ - V^- \cos\!\left(\theta^+ - \theta^-\right)\right) dt. \quad (6)$$

By considering that the voltage normalization scheme is usually adopted to enhance the transient response and the damping of the system, then setting $V^+ = 1\,\mathrm{pu}$ would represent a worst-case condition. To that end, neglecting the cross-coupling term from the negative-sequence control, defining $\delta = \theta^+ - \theta_F^+$, and using that $\theta_F^+ = \int \omega_g \, dt$, (5) can be expressed as

$$\delta = k \int \left(Z_{LT} I^+ \sin\!\left(\phi_{LT} + \theta_I^+\right) - V_F^+ \sin\!\left(\delta^+\right)\right) dt, \quad (7)$$

$$\downarrow$$

$$0 = \dot{\delta} - k\left(Z_{LT} I^+ \sin\!\left(\phi_{LT} + \theta_I^+\right) - V_F^+ \sin\!\left(\delta^+\right)\right). \quad (8)$$

The positive definite Lyapunov candidate function, $V(\delta) = \delta^2$, which satisfies $V(0) = 0$ and $V(\delta) > 0 \;\forall\; \delta \neq 0$ is defined. Here, the superscript $+$ is omitted for convenience. This candidate is radially unbounded and tends to infinity as $|\delta| \to \infty$. To prove global asymptotic stability, the time-derivative of the Lyapunov candidate must be negative definite meaning that $\dot{V}(\delta) < 0 \;\forall\; \delta$. The derivative of the Lyapunov candidate can be shown to be

$$\dot{V}(\delta) = -2kV_F^+ \cos(\delta) \underbrace{\left(Z_{LT} I^+ \sin\!\left(\phi_{LT} + \theta_I^+\right) - V_F^+ \sin(\delta)\right)^2}_{\text{Always positive}}. \quad (9)$$

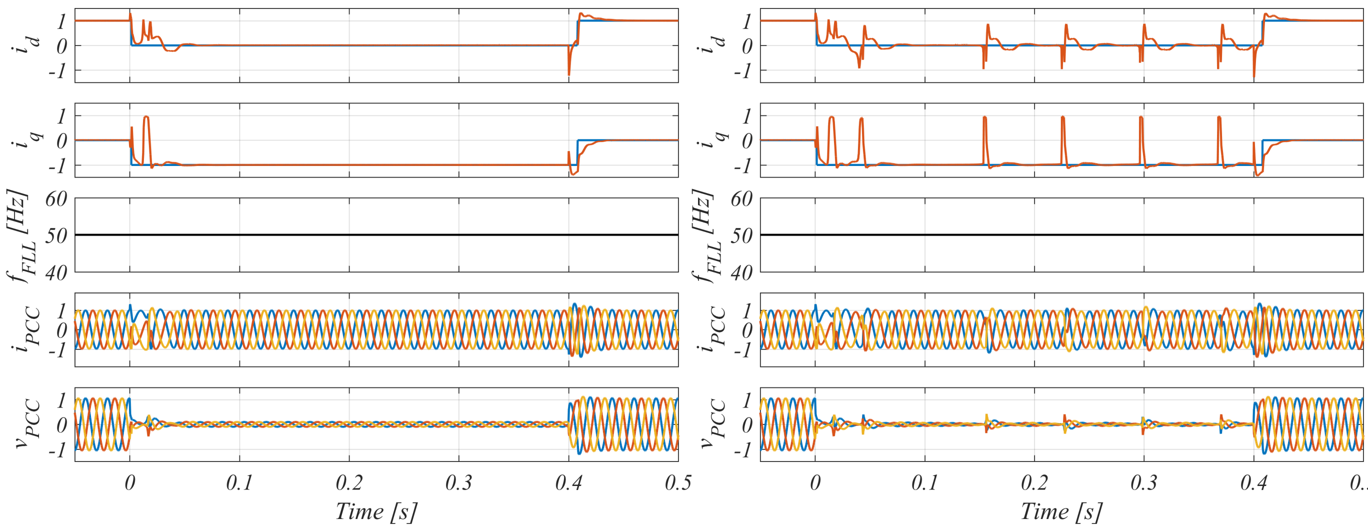

Fig. 4. **Simulation** results for a three-phase symmetrical fault with 1 pu positive-sequence current injection during the fault using the proposed frequency-freezing control. The five subfigures include the d-axis current and its reference, the q-axis current and its reference, the locked FLL frequency, the three-phase PCC currents, and the three-phase PCC voltages. (a): Stable according to (3) with $V_F^+/R_L = 1.01$ (b): Unstable according to (3) with $V_F^+/R_L = 0.99$

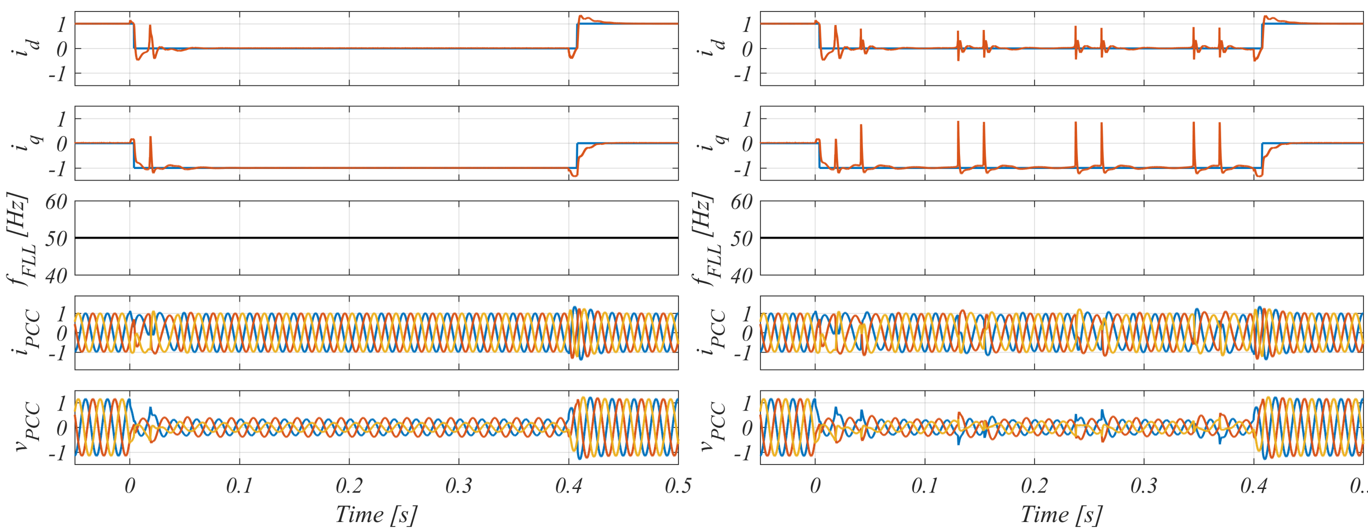

Fig. 5. **Simulation** results for a DLG fault with 1 pu positive-sequence current injection during the fault using the proposed frequency-freezing control. The five subfigures include the d-axis current and its reference, the q-axis current and its reference, the locked FLL frequency, the three-phase PCC currents, and the three-phase PCC voltages. (a): Stable according to (3) with $V_F^+/R_L = 1.01$ (b): Unstable according to (3) with $V_F^+/R_L = 0.99$

Knowing that the control parameter k is positive, then it is satisfied that $\dot{V}(\delta) < 0$ for $\pi/2 > \delta > -\pi/2$, i.e., locally asymptotically stable. However, assuming an equilibrium point to exist during the fault, i.e. (3) is satisfied, then δ will always be in this range. This is true since the synchronization unit is now of first order with $\lambda = 0$, which means that no overshoot will occur in δ when tracking the sagged voltage during the fault. Accordingly, the system is globally asymptotically stable provided that there exists an equilibrium point during the fault and that the cross-coupling term has a negligible effect on the system stability. This conclusion is equally valid for the negative-sequence control. Therefore, it can be appreciated that by using the frequency-freezing control of the DROGI-FLL, this is equivalent to adopting a first-order PLL ignoring the cross-coupling effects in the DROGI-FLL. It should be mentioned that this result is applicable to all stationary-reference frame FLLs where a frequency-adaptive loop is being used. Also, with the similarity between the stationary-reference frame representation and the dq-reference frame representation, this solution for enhanced synchronization stability during grid faults can be achieved by eliminating the integral gain of SRF-PLLs. This particular approach is

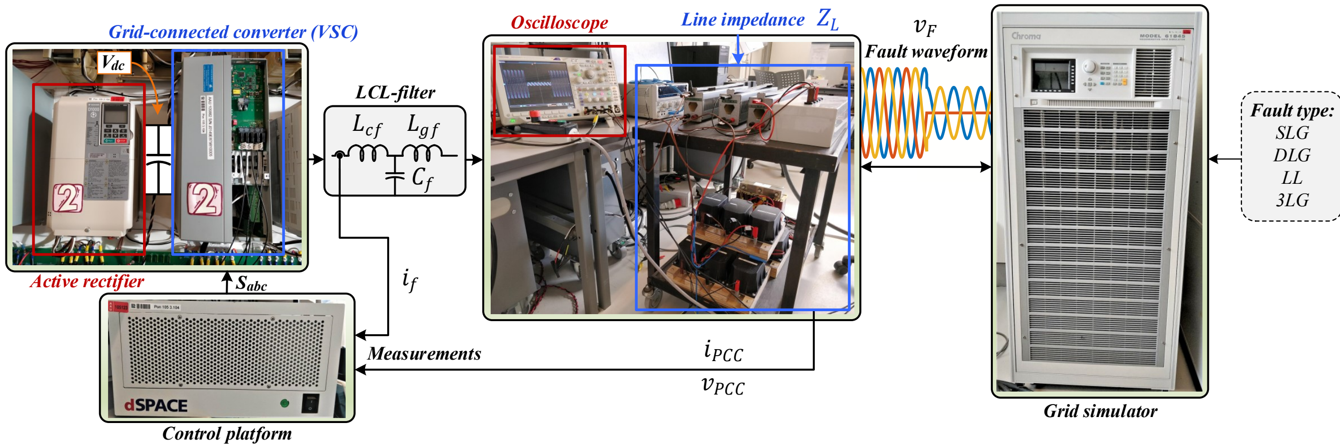

Fig. 6. Laboratory test setup used for the experimental verification. A programmable grid simulator is used to generate the different grid faults, and a grid-connected converter is interfaced through a line impedance. Based on the desired fault type (SLG, DLG, LL, 3LG), one can individually program the dynamical behavior of each phase to emulate different asymmetrical and symmetrical grid faults.

done for an SRF-PLL in [13] where the integral gain of a SRF-PLL is set to zero during grid faults.

Since setting $\lambda = 0$ during the fault reduces the simplified synchronization model to a first-order model, it loses its phase tracking capability if the grid frequency differ from its pre-fault value. To address this issue in low-inertia grids where the frequency may deviate more during imbalances in load and generation, a gain-scheduling approach, as described in [13], may be applied. Here for an SRF-PLL during symmetrical faults, the integral gain is only set to be zero if the rate of change of frequency (RoCoF) is observed to be higher than some defined threshold value. In this way, the first-order PLL is only used if the synchronization is lost or if the defined ROCOF level is violated.

V. Simulation Results and Stability Verification

From the previous section, it is concluded that the proposed frequency-freezing control is globally asymptotically stable, given the existence of a stable intra-fault equilibrium point. This conclusion assumes that the cross-coupling terms in the DROGI-FLL can be neglected. To evaluate the validity of this assumption and the stability of the proposed method, simulation results are performed on the very boarder of the necessary stability condition given in (3). Here, the frequency-freezing control is activated where the necessary stability condition is just met and when it is just violated. In regards to (4), these two considered points are $\frac{V_F^+}{R_L} = 1.01\,\text{pu}$ and $\frac{V_F^+}{R_L} = 0.99\,\text{pu}$, respectively. For the simulation tests, $I^+ = 1\,\text{pu}$, which implies from (4) that the second case is indeed unstable and the first case should be stable according to the stability proof from the previous section.

For a three-phase symmetrical fault, the stable and unstable conditions are shown in Fig. 4. As can be seen from Fig. 4(a), the system stands stable despite of the cross-coupling terms and even though being very close to the theoretical stability boundary. The same tests around the critical stability condition of (4) is conducted for a solid DLG fault as it can be seen in Fig. 5. Again, it is evident that by using the frequency-freezing control, the system can successfully ride through the fault. Therefore, the global asymptotic stability concluded in the previous section is indeed accurate, as the analysis holds sufficiently close to the necessary stability boundary. This also supports that this control method is equivalent to removing the integral action of normal SRF-PLLs as previously performed in [13].

VI. Experimental Results

The test setup used for the experimental verification is shown in Fig. 6, which is designed to have the same parameters as listed in Table I. A grid simulator is used to emulate the short-circuit condition of one or more phases during the fault. Two short-circuit tests are performed to show the validity of the proposed strategy: a three-phase symmetrical fault where the voltage magnitude drops to 0.3 pu and a solid DLG fault, both occurring for 400 ms. These are shown without and with the proposed frequency-freezing control in Fig. 7 and Fig. 8. It is evident that without using the frequency-freezing control of the DROGI-FLL, the loss of synchronization occurs. For the symmetrical fault in Fig. 7(a), it is observed that the converter is nearly disconnected with a low current injection resulting in highly distorted voltages at the PCC. Similarly, for Fig. 8(a), the positive-sequence voltage is unintentionally attenuated, and the negative-sequence voltage is boosted. To that end, the fault recovery process is distorted and prolonged. All of these issues are mitigated by using the proposed frequency-freezing control, as seen in Fig. 7(b) and Fig. 8(b). Accordingly, using the frequency-freezing control ($\lambda = 0$) of FLL-based synchronization units can effectively enhance the transient stability of grid-following converters.

VII. Conclusion

Addressing the issue of transient instability of grid-following converters during grid faults, this article has proposed a method for synchronization units operating un-

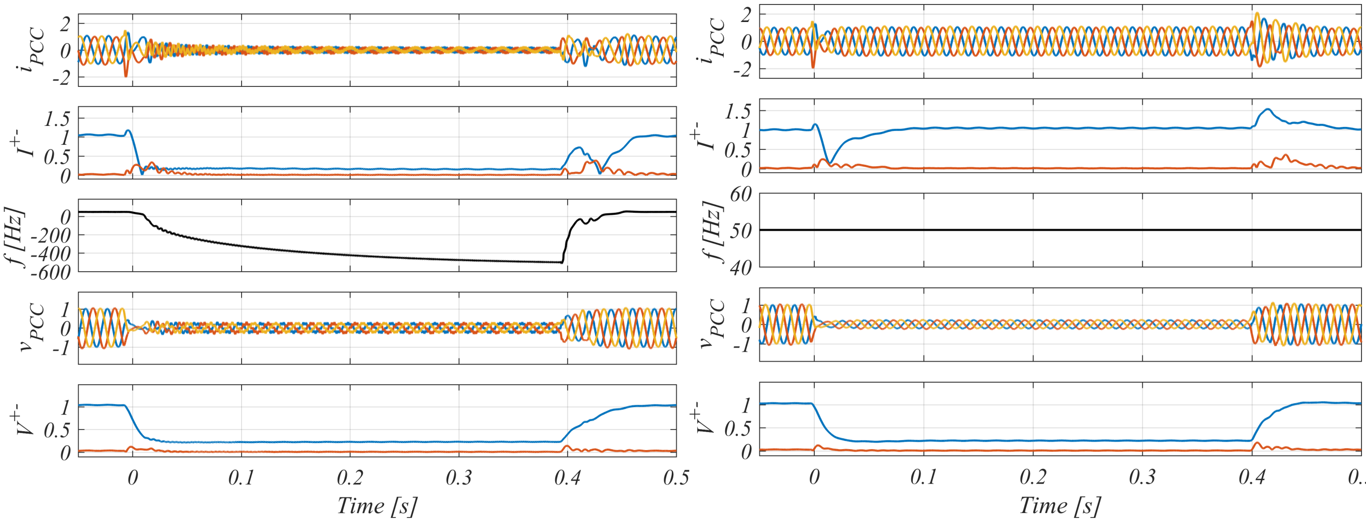

(a) (b)

Fig. 7. **Experimental** results for a three-phase symmetrical fault ($V_F^+ = 0.3\,\mathrm{pu}$) with nominal positive-sequence current injection during fault. (a): Unstable response without the frequency-freezing control. (b): Stable response with proposed frequency-freezing control of the DROGI-FLL.

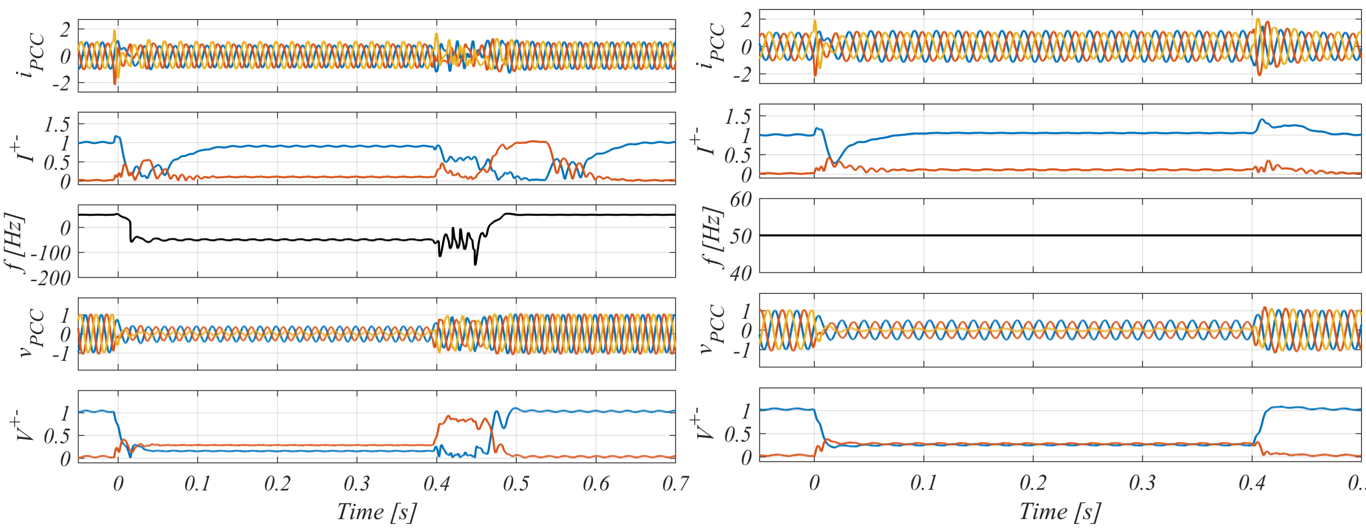

(a) (b)

Fig. 8. **Experimental** results for a DLG fault with nominal positive-sequence current injection during a fault. (a): Unstable response without the frequency-freezing control. (b): Stable response with proposed frequency-freezing control of the DROGI-FLL.

der asymmetrical and symmetrical faults, which by using frequency-freezing control for FLLs, guarantees global asymptotic stability of the system, under the assumption of the existence of an intra-fault equilibrium point. The stability of the proposed method is verified numerically. Additionally, the proposed method is experimentally verified where its robust performance towards severe symmetrical and asymmetrical grid faults is revealed. Furthermore, by showing the equivalence between stationary-reference frequency-locked loops and synchronous-reference phase-locked loops, it has been show that the presented method can be generalized to any FLL or PLL-based synchronization structure and therefore be an appropriate solution in many different applications.

References

[1] NationalGrid, UK, "Performance of phase-locked loop based converters," Tech. Rep., 2017.

[2] Q. Hu, J. Hu, H. Yuan, H. Tang, and Y. Li, "Synchronizing stability of DFIG-based wind turbines attached to weak AC grid," in *Proc. IEEE ICEMS*, Oct 2014, pp. 2618–2624.

[3] M. G. Taul, X. Wang, P. Davari, and F. Blaabjerg, "An overview of assessment methods for synchronization stability of grid-connected converters under severe symmetrical grid faults," *IEEE Trans. Power Electron.*, vol. 34, no. 10, pp. 9655–9670, Oct 2019.

[4] I. Erlich, F. Shewarega, S. Engelhardt, J. Kretschmann, J. Fortmann, and F. Koch, "Effect of wind turbine output current during faults on grid voltage and the transient stability of wind parks," in *Proc. IEEE PESGM*, July 2009, pp. 1–8.

[5] D. Dong, J. Li, D. Boroyevich, P. Mattavelli, I. Cvetkovic, and Y. Xue, "Frequency behavior and its stability of grid-interface converter in distributed generation systems," in *Proc. IEEE APEC*, Feb 2012, pp. 1887–1893.

[6] D. Dong, B. Wen, D. Boroyevich, P. Mattavelli, and Y. Xue, "Analysis of phase-locked loop low-frequency stability in three-phase grid-connected power converters considering impedance interactions," *IEEE Trans. Ind. Electron.*, vol. 62, no. 1, pp. 310–321, Jan 2015.

[7] Q. Hu, L. Fu, F. Ma, and F. Ji, "Large signal synchronizing instability of PLL-based VSC connected to weak AC grid," *IEEE Trans. Power Syst.*, vol. 34, no. 4, pp. 3220–3229, July 2019.

[8] M. G. Taul, X. Wang, P. Davari, and F. Blaabjerg, "Reduced-order and aggregated modeling of large-signal synchronization stability for multiconverter systems," *IEEE J. Emerg. Sel. Topics Power Electron.*, pp. 1–1, 2020.

[9] Ö. Göksu, R. Teodorescu, C. L. Bak, F. Iov, and P. C. Kjær, "Instability of wind turbine converters during current injection to low voltage grid faults and PLL frequency based stability solution," *IEEE Trans. Power Syst.*, vol. 29, no. 4, pp. 1683–1691, July 2014.

[10] S. Ma, H. Geng, L. Liu, G. Yang, and B. C. Pal, "Grid-synchronization stability improvement of large scale wind farm during severe grid fault," *IEEE Trans. Power Syst.*, vol. 33, no. 1, pp. 216–226, Jan 2018.

[11] H. Geng, L. Liu, and R. Li, "Synchronization and reactive current support of PMSG-based wind farm during severe grid fault," *IEEE Trans. Sust. Energy*, vol. 9, no. 4, pp. 1596–1604, Oct 2018.

[12] X. He, H. Geng, R. Li, and B. C. Pal, "Transient stability analysis and enhancement of renewable energy conversion system during LVRT," *IEEE Trans. Sust. Energy*, pp. 1–1, 2019.

[13] H. Wu and X. Wang, "Design-oriented transient stability analysis of pll-synchronized voltage-source converters," *IEEE Trans. Power Electron.*, vol. 35, no. 4, pp. 3573–3589, April 2020.

[14] B. Weise, "Impact of k-factor and active current reduction during fault-ride-through of generating units connected via voltage-sourced converters on power system stability," *IET Renewable Power Generation*, vol. 9, no. 1, pp. 25–36, 2015.

[15] M. G. Taul, X. Wang, P. Davari, and F. Blaabjerg, "Robust fault ride through of converter-based generation during severe faults with phase jumps," *IEEE Trans. Ind. Appl.*, vol. 56, no. 1, pp. 570–583, Jan 2020.

[16] M. G. Taul, R. E. Betz, , and F. Blaabjerg, "Rapid impedance estimation algorithm for mitigation of synchronization instability of paralleled converters under grid faults," in *Proc. IEEE 22nd European Conference on Power Electronics and Applications EPE'20 ECCE Europe*, Sept 2020, pp. 1–5.

[17] N. Tleis, *Power Systems Modelling and Fault Analysis - Theory and Practice*, 1st ed. Elsevier, 2008, ISBN: 978-0-7506-8074-5.

[18] S. Golestan, J. M. Guerrero, and J. C. Vasquez, "Three-phase PLLs: A review of recent advances," *IEEE Trans. Power Electron.*, vol. 32, no. 3, pp. 1894–1907, March 2017.

[19] P. Rodriguez, A. Luna, I. Candela, R. Mujal, R. Teodorescu, and F. Blaabjerg, "Multiresonant frequency-locked loop for grid synchronization of power converters under distorted grid conditions," *IEEE Trans. Ind. Electron.*, vol. 58, no. 1, pp. 127–138, Jan 2011.

[20] P. Rodriguez, J. Pou, J. Bergas, J. I. Candela, R. P. Burgos, and D. Boroyevich, "Decoupled double synchronous reference frame PLL for power converters control," *IEEE Trans. Power Electron.*, vol. 22, no. 2, pp. 584–592, March 2007.

[21] X. Guo, W. Wu, and Z. Chen, "Multiple-complex coefficient-filter-based phase-locked loop and synchronization technique for three-phase grid-interfaced converters in distributed utility networks," *IEEE Trans. Ind. Electron.*, vol. 58, no. 4, pp. 1194–1204, April 2011.

[22] S. Golestan, J. M. Guerrero, and J. C. Vasquez, "High-order frequency-locked loops: A critical analysis," *IEEE Trans. Power Electron.*, vol. 32, no. 5, pp. 3285–3291, May 2017.

[23] S. Golestan, J. M. Guerrero, J. C. Vasquez, A. M. Abusorrah, and Y. Al-Turki, "A study on three-phase FLLs," *IEEE Trans. Power Electron.*, vol. 34, no. 1, pp. 213–224, Jan 2019.

[24] VDE, "VDE-AR-N 4110: Technical requirements for the connection and operation of customer installations to the medium-voltage network (TCC medium-voltage)," 2017.

[25] M. G. Taul, X. Wang, P. Davari, and F. Blaabjerg, "Current reference generation based on next generation grid code requirements of grid-tied converters during asymmetrical faults," *IEEE J. Emerg. Sel. Topics Power Electron.*, pp. 1–1, 2019.

[26] ——, "Systematic approach for transient stability evaluation of grid-tied converters during power system faults," in *Proc. IEEE ECCE*, Sep. 2019, pp. 5191–5198.

[27] S. Golestan, J. M. Guerrero, and J. C. Vasquez, "Is using a complex control gain in three-phase flls reasonable?" *IEEE Trans. Ind. Electron.*, pp. 1–1, 2019.

[28] X. He, H. Geng, J. Xi, and J. M. Guerrero, "Resynchronization analysis and improvement of grid-connected VSCs during grid faults," *IEEE J. Emerg. Sel. Topics Power Electron.*, pp. 1–1, 2019.